

Single-Crystalline LaB₆ Nanowires

Han Zhang,[†] Qi Zhang,[‡] Jie Tang,^{‡,§} and Lu-Chang Qin^{*,†,‡}

Curriculum in Applied and Materials Sciences and Department of Physics and Astronomy, University of North Carolina at Chapel Hill, Chapel Hill, North Carolina 27599-3255, and National Institute for Materials Science, Tsukuba, Japan

Received October 26, 2004; E-mail: lcqin@physics.unc.edu

Lanthanum hexaboride (LaB₆) is widely used in modern technology as an excellent thermionic electron emission source which offers high brightness and long service life. The advantages are originated from its low work function and nature of low volatility.^{1,2} Extensive thermal field-emission tests have also been performed with LaB₆.^{3–5} These studies revealed that, compared to the LaB₆ thermionic electron emitters, a brightness of at least 2 orders of magnitude higher could be achieved with the LaB₆ thermal field emitter. The required local electric field is only half of that needed by the typical commercial thermal field emitters made with zirconiated tungsten sharp tips.

For a LaB₆ thermionic electron emitter, a smaller emitter tip diameter results in a brighter electron beam and a smaller minimum electron beam spot size, which will in turn improve greatly the resolution and performance of electron optical instruments such as the transmission electron microscope (TEM) and the scanning electron microscope (SEM) that are often equipped with a thermionic LaB₆ electron emission cathode.^{6–8} The tip diameter of commercial LaB₆ thermionic electron guns is typically in the range of ~5–100 μm. The emitter tip size plays an even more important role in the thermal field-emission applications such as the Shottky electron gun, which at present is considered as the best high-resolution electron filament. With a low work function as one factor, a strong local electric field is the other factor to determine the electric field-induced emission for a given applied voltage and cathode gun geometry. For a rod-shaped field-induced electron emitter, the local electric field *F* which extracts electrons from the emitter tip can be expressed as a function of the applied voltage *V*, the emitter tip radius *r*, its longitudinal length *h*, and the distance *d* between the anode and the substrate where the emitter stands:⁹

$$F = 1.2V(2.5 + h/r)^{0.9} [1 + 0.013d/(d - h) - 0.033(d - h)/d]$$

The above relationship indicates that the smaller the emitter tip radius *r* and the higher its aspect ratio *h/r*, the greater the local electric field *F* will become, which in turn will enable field-induced electron emission to occur at a lower applied voltage compared to emitters of the same material but of larger dimensions. This lowered turn-on voltage for field-induced electron emission has been observed in many nanoscale structures including carbon nanotubes and nanowires of SiC, W, CuS, and MoO₃ materials.^{10–14} The small diameter and large aspect ratio of such one-dimensional nanostructures magnify enormously the local electric field at the emitter's free end and give greatly enhanced electric field-induced emission from these materials whose work functions are even considered

high compared to that of LaB₆. Therefore, it is of both great scientific and practical significance to fabricate and investigate nanoscale LaB₆, the compound being considered as the best electron emitter material thus far.

We herein report the synthesis and structural characterization of LaB₆ nanowires with diameter smaller than 100 nm and length more than a few tens of micrometers. We have developed and applied a chemical vapor deposition (CVD) method that produces single-crystalline LaB₆ nanowires of uniform diameter and well-defined growth direction. The synthesis is based on the following chemical reaction:^{15–17}



The reaction was conducted in a tube furnace operated at 1150 °C where the BCl₃ gas was introduced to the reaction zone in a stainless steel tube and LaCl₃ powders were vaporized in a tantalum bowl placed inside the tube furnace. The reaction was conducted in an atmosphere at 1 atm pressure of hydrogen and nitrogen (5% H₂ + N₂) gases. Single-crystalline nanowires were grown on gold metal films coated on silicon substrates. Single-crystalline whiskers can also be produced under similar conditions.

For electron diffraction and microscopy observations, the LaB₆ nanowires were first dispersed in ethanol and then collected onto a copper grid that was coated with a thin holey carbon film. The TEM (JEM-2010F equipped with a Shottky field-emission gun) was operated at 200 kV during structural characterization.

A representative morphological study of the nanowires is presented in Figure 1. The nanowires with smooth surfaces of diameter around 100 nm and length extending to more than a few tens of micrometers were observed and measured using both electron imaging and selected-area electron diffraction. Figure 1a is a typical TEM image at low magnification where the dimensional morphology is displayed. Figures 1b–d show three electron diffraction patterns taken from three different crystal zone axes of the same nanowire to identify the LaB₆ crystal lattice, which has a primitive cubic structure of space group *Pm3m* and has lattice constant *a* = 0.4153 nm. The three zone axes are [0 1 -1] (Figure 1b), [-1 2 -1] (Figure 1c), and [-1 4 -2] (Figure 1d). The relative orientational relationship between the three electron diffraction patterns is also given in the figures. For example, the [-1 2 -1] zone axis electron diffraction pattern (Figure 1c) was obtained by rotating the nanowire 30° about its [111] direction (illustrated in Figure 1b). It can also be seen from the diffraction patterns that all reflection spots are elongated to become streaks and these streaks are always perpendicular to the [111] lattice direction, indicating that the nanowire axis is parallel to the [111] direction of the LaB₆ crystal. This result was further confirmed by high-resolution transmission electron microscopy (HRTEM).

HRTEM was applied to analyze the detailed atomic structure around the nanowire tip. Figure 2a is an electron microscope image

[†] Curriculum in Applied and Materials Sciences, University of North Carolina at Chapel Hill.

[‡] Department of Physics and Astronomy, University of North Carolina at Chapel Hill.

[§] National Institute for Materials Science.

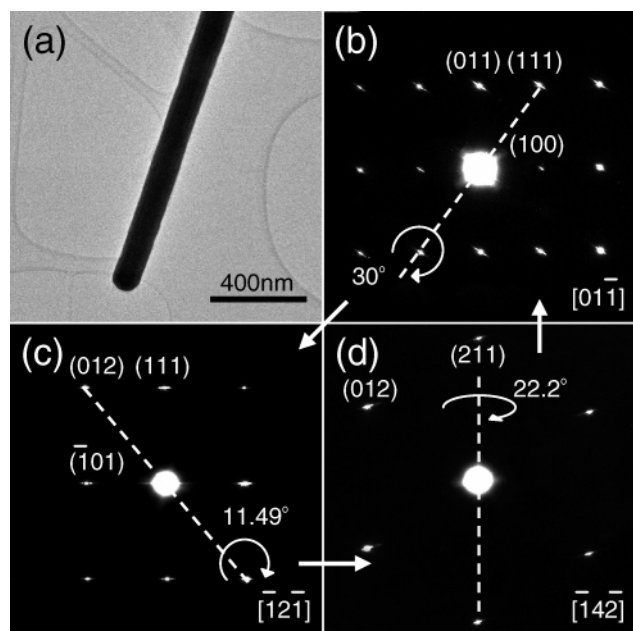


Figure 1. (a) Low-magnification TEM image of a LaB₆ nanowire. (b–d) Electron diffraction patterns of the same LaB₆ nanowire tilted to zone axes [0 1 $\bar{1}$], [$\bar{1}$ 2 $\bar{1}$], and [$\bar{1}$ 4 $\bar{2}$], respectively. Dash lines indicate the tilting axes about which the nanowire was rotated to obtain the needed orientation. Circular arrows give the tilting angles, and the straight arrows point to the tilting sequence.

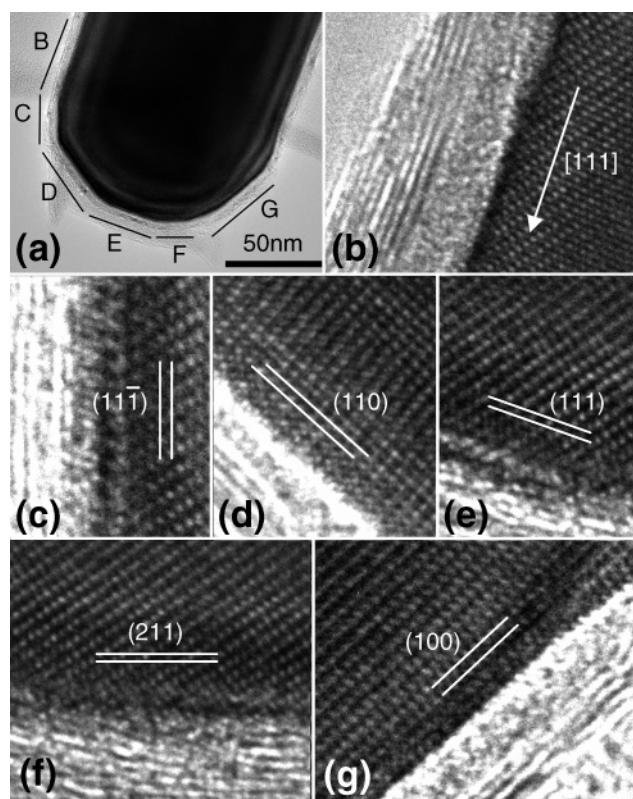


Figure 2. (a) High-resolution image of the LaB₆ nanowire tip with terminating facets labeled with letters B–G. (b–g) Lattice images of the nanowire stem (B) and facets C–G as indicated in (a). The terminating facets are lattice planes of low indices, such as {100} (G), {110} (D), and {111} (C and E).

of the nanowire tip. The tip is hemispherical, and it is terminated by several different lattice planes that are labeled with letters B through G on the image. The HRTEM images characterizing these

faceted lattice planes are displayed in Figures 2b–g in corresponding sequence. Figure 2b shows the lattice image of the stem area (marked B in Figure 2a) of the LaB₆ nanowire. The axial direction, [111], which is the same of the growth direction, of the nanowire has also been indicated in the figure. Figure 2c shows the lattice image near facet C of Figure 2a, whose surface is terminated with the (1 1 $\bar{1}$) lattice plane. Figure 2d shows the area marked with letter D in Figure 2a, which has a (110) facet. Figure 2e shows a (111) facet, which is equivalent to Figure 2c in atomic structure with the same surface energy and is perpendicular to the nanowire axis [111]. Figure 2f shows (211) facet corresponding to the area marked with F in Figure 2a. It is interesting to note that facet F is the smallest compared with others shown in Figure 2a. Area G, shown in Figure 2g, is a facet of (100) which is a low index lattice plane. By examining the areas covered by the various facets characterized, we found that the (100), (110), and (111) planes are the dominant terminating facets. Lattice planes of higher indices appeared only as transitions between the above dominant facet planes of low indices. This result agrees with the lowest surface energy principle in crystal growth.

Though commercial LaB₆ electron gun filaments are usually made along the $\langle 100 \rangle$ direction of the crystal lattice due to the {100} plane's lower work function and higher symmetry,¹ it has been suggested that the $\langle 111 \rangle$ oriented LaB₆ single-crystalline tips might be an even better alternative since they offer better stability.¹⁸ Electric field-induced electron emission measurements on the LaB₆ nanowires are in progress.

In conclusion, we have developed a CVD method that has been able to produce successfully LaB₆ nanowires of well-characterized morphology. The nanowires have a diameter around and smaller than 100 nm and length extending to a few tens of micrometers. The growth direction of the nanowires is its $\langle 111 \rangle$ lattice direction, and they have hemispherical tips that are terminated by lattice planes of low indices such as {100}, {110}, and {111}. The LaB₆ nanowires' potential applications include providing thermionic emission, field-induced emission, and thermal field-induced emission of electrons for TEM, SEM, flat panel displays, as well as other electronic devices that require high-performance electron sources.

References

- (1) Gesley, M.; Swanson, L. W. *Surf. Sci.* **1984**, *146*, 583.
- (2) Swanson, L. W.; Gesley, M.; Davis, P. *Surf. Sci.* **1981**, *107*, 263.
- (3) Harada, K.; Nagata, H.; Shimizu, R. *J. Electron. Microsc.* **1991**, *40*, 1.
- (4) Nagata, H.; Harada, K.; Shimizu, R. *J. Appl. Phys.* **1990**, *68*, 3614.
- (5) Nakamoto, M.; Furuda, K. *Appl. Surf. Sci.* **2002**, *202*, 289.
- (6) Yamabe, M.; Furukawa, Y.; Inagaki, T. *J. Vac. Sci. Technol., A* **1984**, *2*, 1361.
- (7) Doy, T. K.; Kasai, T.; Ohmori, H. *J. Ceram. Soc. Jpn.* **1999**, *107*, 502.
- (8) Tennant, D. M.; Swanson, L. W. *J. Vac. Sci. Technol., B* **1989**, *7*, 93.
- (9) Bonard, J. M.; Dean, K. A.; Coll, B. F.; Klinke, C. *Phys. Rev. Lett.* **2002**, *89*, 197602.
- (10) Rinzler, G.; Hafner, J. H.; Nikolaev, P.; Lou, L.; Kim, S. G.; Tomanek, D.; Nordlander, P.; Colbert, D. T.; Smalley, R. E. *Science* **1995**, *269*, 1550.
- (11) Wong, K. W.; Zhou, X. T.; Au, F. C. K.; Lai, H. L.; Lee, C. S.; Lee, S. T. *Appl. Phys. Lett.* **1999**, *75*, 2918.
- (12) Lee, Y. H.; Choi, C. H.; Jang, Y. T.; Kim, E. K.; Ju, B. K.; Min, N. K.; Ahn, J. H. *Appl. Phys. Lett.* **2002**, *81*, 745.
- (13) Chen, J.; Deng, S. Z.; Xu, N. S.; Wang, S.; Wen, X.; Yang, S.; Yang, C.; Wang, J.; Ge, W. *Appl. Phys. Lett.* **2002**, *80*, 3620.
- (14) Li, Y. B.; Bando, Y.; Golberg, D.; Kurashima, K. *Appl. Phys. Lett.* **2002**, *81*, 5048.
- (15) Motojima, S.; Takahashi, Y.; Sugiyama, K. *J. Cryst. Growth* **1978**, *44*, 106.
- (16) Givargizov, E. I.; Obolenskaya, L. N. *J. Cryst. Growth* **1981**, *51*, 190.
- (17) Givargizov, E. I.; Obolenskaya, L. N. *J. Less-Common Met.* **1986**, *117*, 97.
- (18) Takigawa, T.; Sasaki, I.; Meguro, T.; Motoyama, K. *J. Appl. Phys.* **1982**, *53*, 5891.

JA043512C